Ion migration assisted inscription of high refractive index contrast waveguides by femtosecond laser pulses in phosphate glass

T. Toney Fernandez,[1] P. Haro-González,[2] B. Sotillo,[3] M. Hernandez,[4] D. Jaque,[2] P. Fernandez,[3] C. Domingo,[4] J. Siegel,[1] and J. Solis[1,*]

[1]*Laser Processing Group, Instituto de Optica, CSIC, Serrano 121, 28006-Madrid, Spain*

[2]*Fluorescence Imaging Group, Dep. de Física de Materiales C-IV, Universidad Autónoma de Madrid, C/Francisco Tomás y Valiente 7, Madrid 28049, Spain*

[3]*Depto. de Física de Materiales, Facultad de Físicas, Univ. Complutense, 28040-Madrid, Spain*

[4]*Instituto de Estructura de la Materia, CSIC, Serrano 121, 28006-Madrid, Spain*

**Corresponding author: j.solis@io.cfmac.csic.es*

Received September 10, 2013; revised October 25, 2013; accepted November 4, 2013; posted November 4, 2013 (Doc. ID 197505); published December 4, 2013

In this Letter, we report on the successful fabrication of low loss, high refractive index contrast waveguides via ion migration upon femtosecond laser writing in phosphate glass. Waveguides were produced in two different phosphate glass compositions with high and low La_2O_3 content. In the La-rich glass, a large refractive index increase in the guiding region was observed due to the incoming migration of La accompanied by the out-diffusion of K. The much smaller refractive index change in the La-less glass is caused by rearrangements of the glass structure. These results confirm the feasibility of adapting the glass composition for enabling the laser writing of high refractive index contrast structures via spatially selective modification of the glass composition.

OCIS codes: (320.7090) Ultrafast lasers; (130.2755) Glass waveguides; (160.5690) Rare-earth-doped materials; (180.2520) Fluorescence microscopy.
http://dx.doi.org/10.1364/OL.38.005248

The origin of the refractive index modification caused by femtosecond (fs) laser irradiation in phosphate glasses has been investigated by several research groups. In such reports, mostly commercial glass from Kigre, Inc. (QX and MM2) and Schott AG (IOG) are used [1–5]. Most of these glasses were developed for telecommunication research and industry as base materials for waveguide fabrication by Ag-Na ion exchange [6–8]. With the advent of fs-laser-inscription techniques, demand for new glasses grew even higher due to the ability of fast prototyping and fabrication of complex 3D custom components [5]. Still, little effort was made to optimize the glass composition for this new technique. Due to the versatility of fs-laser writing, many problems were surmounted by adjusting the processing conditions to produce excellent results in various glasses [1,5]. However, there is little doubt that glass composition is a key parameter for further optimizing fs-laser-written optical devices.

Among various commercial phosphate glass compositions, we have identified and isolated a set of glass with and without La_2O_3 to demonstrate the importance of optimizing the glass matrix composition for fs-laser writing. We show that the presence of La_2O_3 enables us to achieve a large positive refractive index contrast (RIC) in the written structures. The responsible mechanism is identified as the migration of La to form a region of increased refractive index accompanied by out-diffusion of K. The compositional changes unambiguously correlate to positive and negative refractive index modifications. Indeed, the refractive index changes observed via La migration are far beyond what can be attributed to changes in the glass structure.

In the present work, we have investigated in detail the role of La_2O_3 in the photo-inscription mechanisms in phosphate glasses. The addition of La_2O_3 to P_2O_5-Al_2O_3 glasses is known to increase the refractive index of the glass [9,10] as well as to improve its thermal, mechanical, and optical properties. We have used two different QX special melt phosphate glass samples from Kigre, Inc., both doped with 2 wt. % Er and 4 wt. % Yb (QX was introduced as a laser glass capable of withstanding high thermal loading and shock). QxErSpa100 ($n = 1.54$ at 1550 nm) has ~10 mol. % La_2O_3 and ~8 mol% of K_2O (*La-rich* sample). QXErSpa47 ($n = 1.51$ at 1550 nm) glass has only 0.4 mol. % La_2O_3 (*La-less* glass). The Al_2O_3 content of both glasses is ~10% mol.

Waveguides were inscribed with a high-repetition-rate fs-laser employing the slit-shaping technique [9,11], using a fiber-based fs-laser amplifier (Tangerine, Amplitude Systems) operating at a wavelength of 1030 nm with a pulse width of 400 fs and an output-beam diameter of 2.0 mm ($1/e^2$ intensity). A 0.68 numerical aperture (NA) aspheric lens was used to focus the laser beam 100 μm underneath the sample surface. Two different slit widths were used for shaping the beam (1.2 and 1.4 mm width). The laser beam was circularly polarized in order to improve waveguide performance [12]. The best waveguide-processing window was found for 500 kHz repetition rate, 500–1000 nJ pulses energies (depending on the slit width and sample) and 40–80 μm/s scan speeds. For phosphate glasses, thermal diffusivities are in the range of $1–6 \times 10^{-3}$ cm^2/s. As a consequence, in our experimental conditions, the effective cooling time, tc [13], is much larger than the time between laser pulses (2 μs). Heat-accumulation effects [14] are thus considerable. After processing, the waveguides were polished and analyzed by means of differential interference

contrast transmission optical microscopy (DIC), microphotoluminescence (μPL), micro-Raman (μ-Raman) and x-ray μ-analysis spectroscopies.

The optical features of the waveguides were first analyzed by DIC. No stress-induced birefringence was observed. In all cases (Fig. 1), the written structures show a characteristic shape with a sharp-pointed, dark region of reduced refractive index and a bright and light guiding, increased refractive index region. The refractive index increase of the guiding region in the La-rich sample has a high contrast with a nearly circular shape (Fig. 1, first row). In La-less glass, it was not possible to produce positive index changes except at higher irradiation energies (>1000 nJ). Given the small differences in optical absorption, we attribute this to the expected higher thermal diffusivity of the La-less glass compared to La-rich glass. By using slit shaping, no better results were obtained in terms of refractive index contrast. Hence moving to a higher repetition rate or a higher fluence (via tighter focusing or higher pulse energy) would be advisable for producing high RIC structures in this glass [1,2].

Figure 1 also shows that by using slit shaping at a high repetition rate, it is feasible to maintain the length of the modified region (‖ to laser direction) over a relatively large fluence range, while the transverse dimension is given by the combination of slit width and fluence. The versatility of using this additional parameter to control the size of the transformed region has clearly been shown in our previous report [9]. The size and RIC obtained for La-rich glass waveguides, written without slit, were large enough to force the input pump mode (980 nm) or both pump and signal mode (1620 nm) to propagate in multimodal behavior (c.f. Fig. 2). Employing slit beam shaping, we were able to control the size of the transformed region, enabling single-mode operation to ensure excellent pump-signal overlap, which is critical for the performance of optical amplifiers. The positive refractive index change (Δn) of the guiding region has been estimated, based on measurements of the NA of the waveguides, to be 1.5×10^{-2} (at 1620 nm). Figure 2 also quotes the propagation losses, which are as low as 0.2 dB/cm. On the contrary, the waveguides fabricated in the La-less glass showed much larger propagation losses (well above 2.5 dB/cm) consistent with previous reports [2].

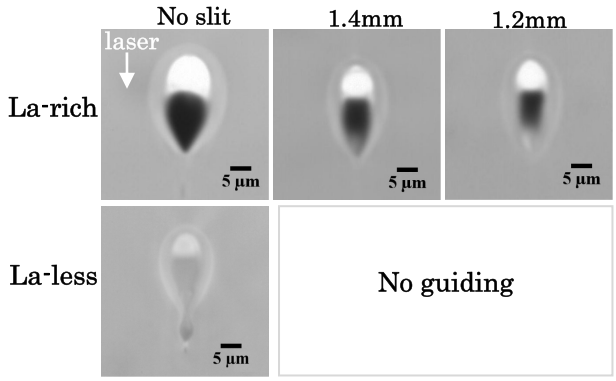

Fig. 1. DIC images of waveguide cross-sections produced in La-rich and La-less phosphate glasses. First row waveguide parameters are 640, 670, and 730 nJ; second row is 1090 nJ. The arrow indicates the writing laser beam propagation direction.

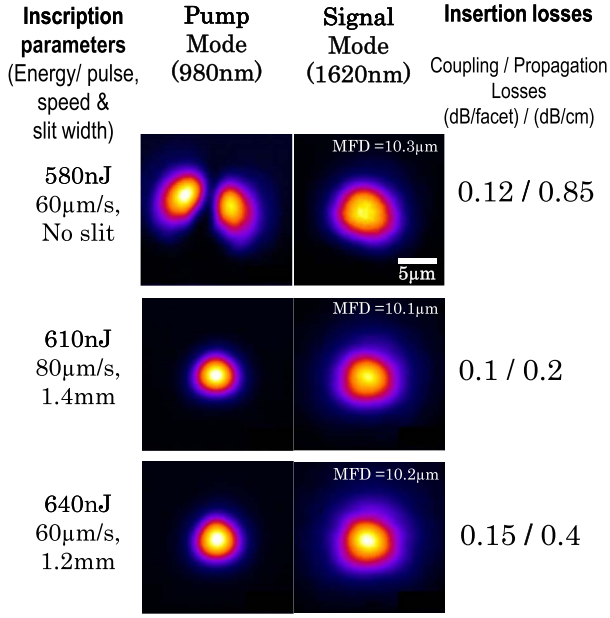

Fig. 2. Mode profiles and insertion losses of the waveguides fabricated in the La-rich glass.

In order to investigate the structural changes occurring in the laser-written structures, we used, in a first stage, μPL [3] and μ-Raman spectroscopy [2]. For the μPL analysis, we used 980 nm laser excitation and analyzed the intensity, peak position, and spectral width of the $^4S_{3/2} \rightarrow {}^4I_{5/2}$ emission of Er ions at 544 nm. This transition is hypersensitive in nature and is ideal for the purpose to indicate changes in the coordination environment of the glass network [15]. Figure 3 shows the μPL-maps of the waveguides corresponding to the green band (540–550 nm) of Er^{3+}. For both glasses, the high refractive index region shows a clear intensity increase, while in the depressed index zone, the emission intensity is found to decrease significantly. The intensity increase in the positive RIC zones for both glasses [Figs. 3(a) and 3(b)] indicates that there is no relevant rare-earth

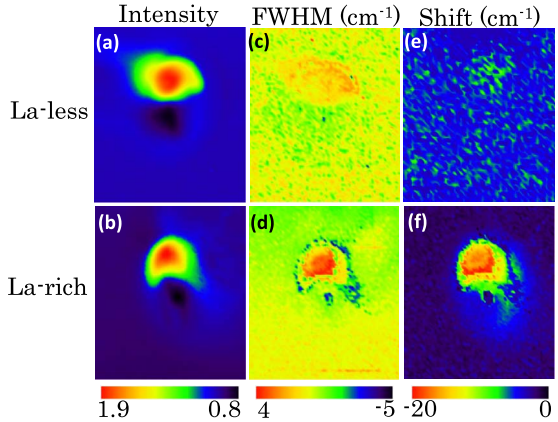

Fig. 3. (a)–(f) Erbium ion green emission (540–550 nm) μPL mappings of waveguides produced in La-less and La-rich phosphate glass. Each image has a dimension of 35 μm × 40 μm. DIC images of both waveguides are shown in the first column of Fig. 1.

clustering or network damage causing fluorescence quenching [15].

The emission spectral width, which can be interpreted in terms of local disorder, is larger in the positive RIC zone for both glasses [Figs. 3(c) and 3(d)]. The strongest difference in the fluorescence images is seen in the spatial variation of the spectral shift of the La-rich sample, indicating a red shift of almost 20 cm^{-1} [Fig. 3(f)]. The waveguide in the La-less sample does not show any appreciable shift [Fig. 3(e)]. The strong red shift in the La-rich glass suggests a large increase of covalency, which is indicative of relatively large local compositional changes (associated to local changes in the La, Al, or K contents) in the guiding region [16]. Since relatively small changes of La_2O_3 content lead to large refractive index changes in phosphate glasses [10], the refractive index increase could be tentatively attributed to the migration of lanthanum or its strong rearrangement in the guiding region. Ion migration can cause P-O bond breakage and subsequent network reconfiguration with the inclusion of modifier ions producing a strong and extensive covalent network.

Complementary information regarding local rearrangements of the glass structure was obtained by Raman spectroscopy. The micro-Raman spectra were performed with an excitation wavelength of 442 nm using a Renishaw inVia Raman microscope with 50× (0.75 NA) focusing optics, leading to a spatial resolution <1 μm. The recorded Raman spectra in the La-less sample were essentially identical to those reported in [2] for MM2-glass, dominated by the (PO_2) symmetric vibration band at 1209 cm^{-1} [Fig. 4(a)]. Systematic shifts in this Raman peak to lower and higher wavenumbers have been related by Fletcher *et al.* to an overall expansion/contraction of the phosphate network [2]. In our case, the maximum Raman peak shift of the $(PO_2)_{sym}$ vibration from the negative to the positive refractive index regions was ~6 cm^{-1}, which is consistent with the values reported in [2] with a maximum refractive index change in the $\sim 10^{-3}$ range.

In the La-rich glass, the $(PO_2)_{sym}$ band is observed at 1178 cm^{-1} due to the presence of La_2O_3 [10]. Interestingly, the maximum peak shift observed is just ~3.5 cm^{-1} as shown in Fig. 4(b). The comparison of this value with the observations in the La-less sample suggests that the structural changes associated to this peak shift cannot fully explain the very large positive index in the La-rich sample. The map [Fig. 4(b)] also evidences that the spatial extension of the region where the $(PO_2)_{sym}$ is shifted to higher energies (densified region) is much smaller than the guiding region itself, which also supports the need for an alternative mechanism to explain the large, positive refractive index change in this sample. Finally, along with the indicated features, the relative intensity of $(PO_2)_{asym}$ band at ~1240 cm^{-1} is observed to increase in the positive RIC zone [Fig. 4(c)], which would indicate a higher level of disorder than in the nonirradiated region, in agreement with the observed increase of fluorescence emission bandwidth described above [Fig. 3(d)].

Globally, the above results (μPL and μ-Raman) strongly suggest the existence of large compositional changes in the guiding region of waveguides fabricated in the La-rich glasses. This hypothesis has been confirmed by means of energy-dispersive x-ray μ-analysis measurements in a Leica S440 SEM equipped with a Bruker AXS Quantax μ-analysis system with a resolution of 125 eV. As shown in Fig. 5(a), at first glance, the contrast of the structure in the secondary electron image already evidences a strong Z contrast, which confirms the enrichment of the guiding region with heavy elements and their depletion in the low refractive index zone. On the contrary, in the waveguides of the La-less sample, a weaker Z contrast was observed.

The compositional map of the waveguides produced in the La-rich sample evidenced a quite homogeneous increase of La concentration [Fig. 5(b)] in the high refractive index region of the order of ~25% [relative to the La conc. in the un-irradiated material, Fig. 5(c)]. Relative changes in the x-ray signal associated to a given element of about 0.5% can be differentiated from the intrinsic noise of the measurement, indicating a real change in its concentration. This large enrichment in La is accompanied by the cross migration of K to the low refractive index zone that increases its local concentration by a similar amount [Fig. 5(c)]. We also see a smaller depletion of P in the high refractive index zone. Changes

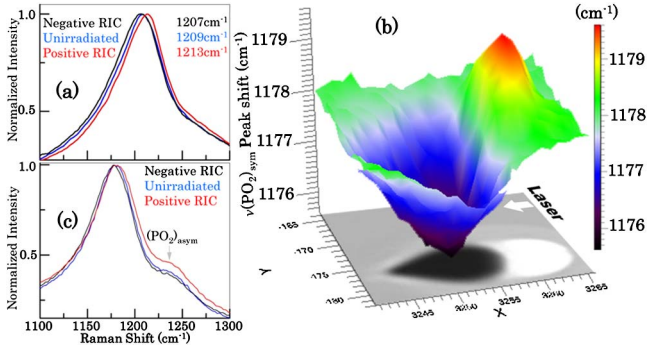

Fig. 4. (a) and (c) PO_2 vibration bands in La-less and La-rich glasses, respectively. (b) 2D mapping of the PO_2 symmetric vibration Raman peak position (cm^{-1}) in the waveguide inscribed in La-rich glass. The image at the base of the plot corresponds to DIC-optical transmission micrograph of the structure showing the (bright) light guiding region. The horizontal scales are in micrometers.

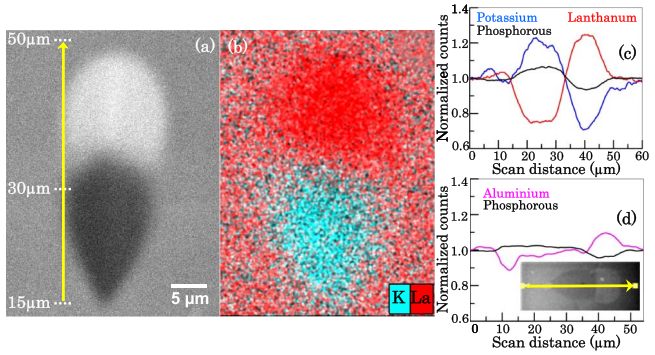

Fig. 5. (a) Secondary electron image of a waveguide fabricated in the La-rich glass. Yellow arrow marks the corresponding scan distance in 5(c) line scan. (b) EDX mapping showing the distribution of La (red) and K (cyan) in the irradiated region. (c) and (d) Line scans of combined ion migrations in La-rich and La-less glass, respectively.

in the Al concentration are below experimental resolution. In the case of La-phosphate glasses, it has been shown [10] that, within the low compositional region $0 < La_2O_3 < 15$ mol%, the density and refractive index of the glass increase linearly with the La_2O_3 content (Δn per mole fraction of $La_2O_3 \approx 4.9 \times 10^{-3}$) mainly because of the relative mass of the La^{3+} ions and that the relatively small size of the isolated La-polyhedra can be easily accommodated by the phosphate network. In our case, for the observed relative increase of 25% [Fig. 5(c)] in the La content, a $\Delta n \approx 1.22 \times 10^{-2}$ could be predicted, which is in very good agreement with 1.5×10^{-2} value obtained from the NA measurements. In the La-less sample, there is also a similar P depletion accompanied by the cross migration of Al, which is enriched by 10% [Fig. 5(d)] in the high refractive index zone. The Al enrichment seems to have little effect in refractive increase induced, more related to changes in the glass network (Fig. 4).

Radial ion migration upon static irradiation of glass at energies near/above the damage threshold [17] and more similar element cross-diffusion effects upon waveguide inscription in glass [18] have been reported before upon HRR fs-laser irradiation. However, the observed diffusion effects had no effect on the RIC induced. We observe that the single valence ions (K^+, $P^{+,+3}$) apparently tend to move codirectional to the incoming laser beam and toward the focal point, while multivalence ions (La^{3+}, Al^{3+}) would move vice-versa. Such tendency would be consistent with the results reported in [18] (K^+, Na^+ single valence and $Si^{2+,4+}$, Zn^{2+} multivalence ions). As for the migration direction being along the laser propagation axis, Luo *et al.* were able to relate it to the axially nonsymmetric energy-deposition profiles and even invert the migration direction [19]. Further experiments in other glass compositions are currently being carried out to confirm this tendency.

In summary, we have fabricated optical waveguides in phosphate glasses, with and without lanthanum oxide as glass modifier, using the femtosecond laser inscription technique. It was observed that strong laser-induced cross migration involving La and K ions forms the basis of the creation of high refractive index areas in the surroundings of laser-writing focus. The feasibility of incorporating La_2O_3 as a glass modifier, along with K_2O or Na_2O, in other glass compositions may potentially lead to the production of highly efficient light-guiding structures with large refractive index contrasts helping to produce high-density 3D optical network waveguides with large bend-radius and negligible losses.

This work was partially supported by the Spanish Ministry Economy and Competitiveness (TEC2011-22422), Spanish Ministerio de Educacion y Ciencia (MAT2010-16161), MINECO (Projects MAT 2012-31959 and CSD2009-00013), and the JAE-CSIC Program (TTF). We thank F. Muñoz (ICV-CSIC, Madrid, Spain) for fruitful discussions on phosphate glasses.

References

1. R. Osellame, N. Chiodo, G. Della Valle, G. Cerullo, R. Ramponi, P. Laporta, A. Killi, U. Morgner, and O. Svelto, IEEE J. Sel. Top. Quantum Electron. **12**, 277 (2006).
2. L. B. Fletcher, J. J. Witcher, W. B. Reichman, A. Arai, J. Bovatsek, and D. M. Krol, J. Appl. Phys. **106**, 083107 (2009).
3. A. Ferrer, D. Jaque, J. Siegel, A. R. de la Cruz, and J. Solis, J. Appl. Phys. **109**, 093107 (2011).
4. D. J. Little, M. Ams, P. Dekker, G. D. Marshall, and M. J. Withford, J. Appl. Phys. **108**, 033110 (2010).
5. R. Osellame, G. Cerullo, R. Ramponi, and G. Valle, in *Femtosecond Laser Micromachining: Photonic and Microfluidic Devices in Transparent Materials* (Springer, 2012), pp. 265–292.
6. G. Della Valle, S. Taccheo, P. Laporta, G. Sorbello, E. Cianci, and V. Foglietti, Electron. Lett. **42**, 632 (2006).
7. http://www.schott.com/advanced_optics/english/download/schott-iog-1-phosphate-laser-glass-may-2013-eng.pdf.
8. http://www.kigre.com/files/mm2data.pdf.
9. J. Hoyo, V. Berdejo, T. T. Fernandez, A. Ferrer, A. Ruiz, J. A. Valles, M. A. Rebolledo, I. Ortega-Feliu, and J. Solis, Laser Phys. Lett. **10**, 105802 (2013).
10. R. K. Brow, E. Metwalli, and D. L. Sidebottom, in *Inorganic Optical Materials II*, A. J. Marker III and E. G. Arthurs, eds. (SPIE, 2000), pp. 88–94.
11. Y. Cheng, K. Sugioka, K. Midorikawa, M. Masuda, K. Toyoda, M. Kawachi, and K. Shihoyama, Opt. Lett. **28**, 55 (2003).
12. M. Ams, G. D. Marshall, and M. J. Withford, Opt. Express **14**, 13158 (2006).
13. S. Juodkazis, H. Misawa, and I. Maksimov, Appl. Phys. Lett. **85**, 5239 (2004).
14. S. Eaton, H. Zhang, P. Herman, F. Yoshino, L. Shah, J. Bovatsek, and A. Arai, Opt. Express **13**, 4708 (2005).
15. K. Shinozaki, A. Noji, T. Honma, and T. Komatsu, J. Fluorine Chem. **145**, 81 (2013).
16. H. Takebe, Y. Nageno, and K. Morinaga, J. Am. Ceram. Soc. **77**, 2132 (1994).
17. Y. Liu, M. Shimizu, B. Zhu, Y. Dai, B. Qian, J. Qiu, Y. Shimotsuma, K. Miura, and K. Hirao, Opt. Lett. **34**, 136 (2009).
18. P. Mardilovich, L. B. Fletcher, N. W. Troy, L. Yang, H. Huang, S. H. Risbud, and D. M. Krol, Int. J. Appl. Glass Sci. **4**, 87 (2013).
19. F. Luo, J. Song, X. Hu, H. Sun, G. Lin, H. Pan, Y. Cheng, L. Liu, J. Qiu, Q. Zhao, and Z. Xu, Opt. Lett. **36**, 2125 (2011).